

Leak Detection, Size Estimation and Localization in Pipe Flows

Ole Morten Aamo, *Member, IEEE*

Abstract—We design a leak detection system consisting of an adaptive observer based on a set of two coupled one dimensional first order hyperbolic partial differential equations governing the flow dynamics. It is assumed that measurements are only available at the inlet and outlet of the pipe. Convergence properties are provided showing that the leak size estimation problem can be tackled independently from how the leak is distributed along the pipe. This is key to obtaining a simple estimation scheme for the leak location. Simulations are provided to demonstrate the ability of the system to detect, quantify and locate leaks.

Index Terms—Distributed parameter systems, fluid flow systems, leak detection, linear systems.

I. INTRODUCTION

Transportation of fluids in pipelines requires monitoring to detect malfunctioning such as leaks. In the petroleum industry, leaks from pipelines may potentially cause environmental damage, as well as economic loss. These are motivating factors, along with requirements from environmental authorities, for developing efficient leak detection systems. Several companies offer commercial solutions to pipeline monitoring with leak detection. While some leak detection methods are hardware-based, relying on physical equipment being installed along the pipeline, the focus of this technical note is software-based methods that work for cases with limited instrumentation. We will restrict the instrumentation to pressure and flow measurements at the inlet and outlet of the pipeline, only. This calls for sophisticated signal processing methods to obtain reliable detection of leaks. Some software-based leak detection methods perform statistical analysis on measurements (black box), while others incorporate models based on physical principles. Our method falls into the latter category, in that we will use a dynamic model of the pipe flow based on a set of two coupled hyperbolic partial differential equations. A recent survey on leak detection techniques is provided in [1]. In that paper, available leak detection algorithms are divided into no less than 13 distinct categories (!), one of which is labeled “Real time transient modelling” and encompasses our model-based approach.

There have been several studies on model-based leak detection. We mention here the most relevant ones with regard to our work. Based on a discretized pipe flow model, an observer with friction adaptation was designed in [2]. In the event of a leak, the outputs from the observer differs from the measurements, and this is exploited in a correlation technique that detects, quantifies and locates the leak. In [3], a bank of observers was used, computed by the method for fault detection and isolation developed in [4]. The underlying model is a linearized, discretized pipe flow model on a grid of N nodes. The

observers are designed in such a way that all but one will react to a leak. Which one of the N observers that does not react to the leak depends on the location of the leak, and this is the mechanism by which the leak is located. The outputs of the remaining observers are used for quantifying the leak. The bank of observers are computed using the recursive numerical procedure suggested in [4], however it was shown in [5] that due to the simple structure of the discretized model, the observers may be written explicitly. This is important, because it removes the need for recomputing the bank of observers when the operating point of the pipeline is changed. In [6], a nonlinear version was proposed, using an extremely coarse discretization grid. The detection method presented in [3], [6], using a bank of observers, can potentially detect multiple leaks. However, multiple simultaneous leaks is an unlikely event, so the complex structure of a bank of N observers seems unnecessary. Thus, in [7], we instead employed ideas from adaptive control, treating the size and location of a single point leak as constant unknown parameters in an adaptive Luenberger-type observer based on a set of two coupled one dimensional first order hyperbolic partial differential equations. Heuristic update laws for adaptation of the friction coefficient, size of the leak and location of the leak were suggested. The method was refined further in [8], [9], and even extended to two-phase flow in [10], but the update laws remained heuristic. In the present technical note, we provide detection, estimation and localization algorithms with rigorous convergence proofs. To our knowledge, this is the first rigorous convergence proof for leak size and localization in an infinite-dimensional hydraulic flow model. It is accomplished using recent advances in observer design by backstepping for partial differential equations of hyperbolic type, presented in [11]–[13], along with the novel contributions of Lemma 1, Lemma 5, and Section III-B. Lemma 1 provides a transformation of the system dynamics into a form that is independent of the location of the leak and at the same time allows straight forward application of the results in [11]–[13]. Lemma 5 provides an additional technical convergence result pertaining to the observer presented in [11], [13] that is needed for developing the localization results of Section III-B. Results from [19] are employed to obtain observer gains in closed form, which significantly simplifies the observer and the numerics involved in its implementation.

The results of the present technical note are formulated for fluid transport in pipelines, but can easily be modified for other relevant applications. Examples are leak detection in open water irrigation channels [14] and kick or loss detection in oil well drilling operations [15]–[17].

II. PIPELINE MODELLING

The 1-dimensional equations of mass conservation and momentum conservation for single phase fluid flow in a pipe of length l are given as [18]

$$p_t(z, t) = -\frac{\beta}{A} q_z(z, t) - \frac{\beta}{F} d(z) \chi \quad (1)$$

$$q_t(z, t) = -\frac{\rho}{\rho} p_z(z, t) - \frac{1}{\rho} q(z, t) - Ag \sin \theta(z) - \frac{1}{A} d(z) \chi^2 \quad (2)$$

$$q_0(0, t) = q_0(t), \quad p(l, t) = p_l(t) \quad (3)$$

Manuscript received July 21, 2014; revised December 19, 2014, December 20, 2014, and April 27, 2015; accepted May 3, 2015. Date of publication May 15, 2015; date of current version December 24, 2015. Recommended by Associate Editor C. Prieur.

The author is with the Department of Engineering Cybernetics, Norwegian University of Science and Technology, Trondheim N-7491, Norway (e-mail: aamo@ntnu.no).

Color versions of one or more of the figures in this paper are available online at <http://ieeexplore.ieee.org>.

Digital Object Identifier 10.1109/TAC.2015.2434031

where $z \in [0, l]$, $t \geq 0$, $p(z, t)$ is pressure, $q(z, t)$ is volumetric flow, β is the bulk modulus of the fluid, ρ is the density of the fluid, A is the cross sectional area of the pipe, F is the friction factor, g is the acceleration of gravity, and $\theta(z)$ is the inclination angle of the pipeline at location z . The subscripts t and z denote partial derivatives. The last terms in (1) and (2) characterize a leak, where χ is the total leak size over the pipeline, and $d(z)$ defines the distribution of the leak as a function of z . We assume that χ is constant and positive and that $d(z)$ satisfies

$$d(z) \geq 0, \forall z \in [0, l], \int_0^l d(\gamma) d\gamma = 1. \quad (4)$$

Defining

$$\delta(z) = l - z - \int_z^l \int_0^\eta d(\gamma) d\gamma d\eta \quad (5) \quad \text{with}$$

we have

$$p_t(z, t) = -\frac{\beta}{A} q_z(z, t) - \frac{\beta}{A} \delta''(z) \chi, \quad (6)$$

$$q_t(z, t) = -\frac{A}{\rho} p_z(z, t) - \frac{F}{\rho} q(z, t) - Ag \sin \theta(z) - \frac{1}{A} \delta''(z) \chi^2, \quad (7)$$

$$q(0, t) = q_0(t), \quad p(l, t) = p_l(t). \quad (8)$$

We assume that flow and pressure at the inlet and the outlet of the pipeline are the only available measurements. They are denoted $q_0(t)$, $p_0(t)$, $q_l(t)$ and $p_l(t)$.

III. MAIN RESULTS

A. Estimation of Leak Size

The key to estimation of leak size is to transform system (6)–(8) into the form used for observer design in [13], where a disturbance—which in the present case will be the leak—enters at the boundary. Lemma 1 accomplishes this. Then, results from [13] are applied to establish convergence of states and leak size to their true values. For completeness the results needed from [13] are re-stated in Lemmas 2 and 3, along with some intermediate derivations needed for a new convergence result for the boundary values of the state, which is given in Lemma 5. While Lemma 5 plays no part in the main result on leak size estimation, it is needed for leak localization in Section III-B. To accomodate simple implementation of the observer, we use results from [19] to provide observer gains in closed form. They are given in Corollary 7 which follows from Lemma 6. These intermediate results lead to the main result on leak size estimation, which is stated in Theorem 8.

Lemma 1: The coordinate transformation

$$u(x, t) = \frac{1}{2} (q(xl, t) - q_{in} + \delta'(xl) \chi + \frac{A}{\sqrt{\beta\rho}} \left(p(xl, t) - p_{out} + \rho g \int_0^{xl} \sin \theta(\gamma) d\gamma + \frac{F}{A} q_{in} xl + \frac{\rho}{A^2} \delta'(xl) \chi^2 - \frac{F}{A} \delta(xl) \chi \right) e^{\frac{lF}{2\sqrt{\beta\rho}} x} \quad (9)$$

$$v(x, t) = \frac{1}{2} (q(xl, t) - q_{in} + \delta'(xl) \chi - \frac{A}{\sqrt{\beta\rho}} \left(p(xl, t) - p_{out} + \rho g \int_0^{xl} \sin \theta(\gamma) d\gamma + \frac{F}{A} q_{in} xl + \frac{\rho}{A^2} \delta'(xl) \chi^2 - \frac{F}{A} \delta(xl) \chi \right) e^{-\frac{lF}{2\sqrt{\beta\rho}} x} \quad (10)$$

for $x \in [0, 1]$, maps (6)–(8) into

$$u_t(x, t) = -\epsilon_1 u_x(x, t) + c_1(x) v(x, t), \quad (11)$$

$$v_t(x, t) = \epsilon_2 v_x(x, t) + c_2(x) u(x, t), \quad (12)$$

$$u(0, t) = \kappa v(0, t) + q_0(t) - q_{in} - \chi, \quad (13)$$

$$v(1, t) = U(t) \quad (14)$$

$$\epsilon_1 = \epsilon_2 = \frac{1}{l} \sqrt{\frac{\beta}{\rho}}, \quad \kappa = -1 \quad (15)$$

$$c_1(x) = -\frac{1}{2} \frac{F}{\rho} e^{\frac{lF}{\sqrt{\beta\rho}} x}, \quad c_2(x) = -\frac{1}{2} \frac{F}{\rho} e^{-\frac{lF}{\sqrt{\beta\rho}} x} \quad (16)$$

$$U(t) = \frac{1}{2} e^{-\frac{lF}{2\sqrt{\beta\rho}}} (q_l(t) - q_{in} - \frac{A}{\sqrt{\beta\rho}} \left(p_l(t) - p_{out} + \rho gh + \frac{Fl}{A} q_{in} \right)) \quad (17)$$

and

$$h = \int_0^l \sin \theta(\gamma) d\gamma. \quad (18)$$

Proof: The result is verified by substituting the inverse of (9), (10) into (6)–(8) to obtain (11)–(14). ■

The parameters q_{in} and p_{out} appearing in Lemma 1 are arbitrary constants that can be used to shift the origin of (u, v) to align with a desired operating point. They serve no other purpose, and may be omitted. The significance of the Lemma is twofold. On the one side it facilitates application of the backstepping method, allowing us to exploit several previous results. But equally important is the fact that it renders the system dynamics independent of the distribution of the leak, which is in general an unknown function of z . This enables a remarkably simple estimation scheme for localization of the leak, as shown in Section III-B. Having established that the pipeline model takes the form (11)–(14), we can apply the results from [13]. Consider the observer

$$\hat{u}_t(x, t) = -\epsilon_1 \hat{u}_x(x, t) + c_1(x) \hat{v}(x, t) + p_1(x) (Y(1, t) - \hat{u}(1, t)) \quad (19)$$

$$\hat{v}_t(x, t) = \epsilon_2 \hat{v}_x(x, t) + c_2(x) \hat{u}(x, t) + p_2(x) (Y(1, t) - \hat{u}(1, t)) \quad (20)$$

$$\hat{u}(0, t) = \kappa \hat{v}(0, t) + q_0(t) - q_{in} - \hat{\chi}(t) \quad (21)$$

$$\hat{v}(1, t) = U(t) \quad (22)$$

$$\dot{\hat{\chi}}(t) = L (Y(1, t) - \hat{u}(1, t)) \quad (23)$$

where

$$Y(1, t) = u(1, t) = \frac{1}{2} e^{\frac{lF}{2\sqrt{\beta\rho}}} (q_l(t) - q_{in} + \frac{A}{\sqrt{\beta\rho}} \left(p_l(t) - p_{out} + \rho gh + \frac{Fl}{A} q_{in} \right)) \quad (24)$$

which is derived from (9) and the fact that $\delta(l) = \delta'(l) = 0$. The functions $p_1(x)$ and $p_2(x)$, and the constant L are output injection gains. Forming error equations by subtracting (19)–(23) from (11)–(14), we have

$$\begin{aligned} \tilde{u}_t(x, t) &= -\epsilon_1 \tilde{u}_x(x, t) + c_1(x) \tilde{v}(x, t) \\ &\quad - p_1(x) \tilde{u}(1, t) \end{aligned} \quad (25)$$

$$\begin{aligned} \tilde{v}_t(x, t) &= \epsilon_2 \tilde{v}_x(x, t) + c_2(x) \tilde{u}(x, t) \\ &\quad - p_2(x) \tilde{u}(1, t) \end{aligned} \quad (26)$$

$$\tilde{u}(0, t) = \kappa \tilde{v}(0, t) - \tilde{\chi}(t) \quad (27)$$

$$\tilde{v}(1, t) = 0 \quad (28)$$

$$\dot{\tilde{\chi}}(t) = -L \tilde{u}(1, t). \quad (29)$$

In [11], the following backstepping transformation

$$\begin{aligned} \tilde{u}(x, t) &= \tilde{\alpha}(x, t) - \int_x^1 P^{uu}(x, \xi) \tilde{\alpha}(\xi, t) d\xi \\ &\quad - \int_x^1 P^{uv}(x, \xi) \tilde{\beta}(\xi, t) d\xi \end{aligned} \quad (30)$$

$$\begin{aligned} \tilde{v}(x, t) &= \tilde{\beta}(x, t) - \int_x^1 P^{vu}(x, \xi) \tilde{\alpha}(\xi, t) d\xi \\ &\quad - \int_x^1 P^{vv}(x, \xi) \tilde{\beta}(\xi, t) d\xi \end{aligned} \quad (31)$$

was used for observer design in the case without χ entering at the boundary, where the kernels are given by the system of equations

$$\epsilon_1 P_x^{uu}(x, \xi) + \epsilon_1 P_\xi^{uu}(x, \xi) = c_1(x) P^{vu}(x, \xi) \quad (32)$$

$$\epsilon_1 P_x^{uv}(x, \xi) - \epsilon_2 P_\xi^{uv}(x, \xi) = c_1(x) P^{vv}(x, \xi) \quad (33)$$

$$\epsilon_2 P_x^{vu}(x, \xi) - \epsilon_1 P_\xi^{vu}(x, \xi) = -c_2(x) P^{uu}(x, \xi) \quad (34)$$

$$\epsilon_2 P_x^{vv}(x, \xi) + \epsilon_2 P_\xi^{vv}(x, \xi) = -c_2(x) P^{uv}(x, \xi) \quad (35)$$

on $\mathcal{T}_o = \{(x, \xi) : 0 \leq x \leq \xi \leq 1\}$ with boundary conditions

$$P^{uu}(0, \xi) = \kappa P^{vu}(0, \xi) \quad (36)$$

$$P^{uv}(x, x) = \frac{c_1(x)}{\epsilon_1 + \epsilon_2} \quad (37)$$

$$P^{vu}(x, x) = -\frac{c_2(x)}{\epsilon_1 + \epsilon_2} \quad (38)$$

$$P^{vv}(0, \xi) = \frac{1}{\kappa} P^{uv}(0, \xi). \quad (39)$$

It was shown in [11] that there exists a unique solution to (32)–(39) which is $C(\mathcal{T}_o)$. We have the following result for our error system (25)–(29).

Lemma 2 ([13, Lemma 6]): Let $(P^{uu}, P^{uv}, P^{vu}, P^{vv})$ be the solution to (32)–(39). The transformation (30), (31) maps the system

$$\tilde{\alpha}_t(x, t) = -\epsilon_1 \tilde{\alpha}_x(x, t) + L \tilde{\alpha}(1, t) \quad (40)$$

$$\tilde{\beta}_t(x, t) = \epsilon_2 \tilde{\beta}_x(x, t) \quad (41)$$

with boundary conditions

$$\tilde{\alpha}(0, t) = \kappa \tilde{\beta}(0, t) - \tilde{X}(t) \quad (42)$$

$$\tilde{\beta}(1, t) = 0 \quad (43)$$

and

$$\dot{\tilde{X}}(t) = -L \tilde{\alpha}(1, t) \quad (44)$$

into (25)–(29) with

$$p_1(x) = -L - \epsilon_1 P^{uu}(x, 1) + L \int_x^1 P^{uu}(x, \xi) d\xi \quad (45)$$

$$p_2(x) = -\epsilon_1 P^{vu}(x, 1) + L \int_x^1 P^{vu}(x, \xi) d\xi. \quad (46)$$

It was shown in [11] that the transformation (30), (31) is invertible, so that stability properties of (25)–(29) and (40)–(44) are equivalent. It is clear from (41) and (43) that $\tilde{\beta}(x, t)$ converges to 0 in finite time, so it suffices to consider stability of the origin of

$$\tilde{\alpha}_t(x, t) = -\epsilon_1 \tilde{\alpha}_x(x, t) + L \tilde{\alpha}(1, t) \quad (47)$$

$$\tilde{\alpha}(0, t) = -\tilde{X}(t) \quad (48)$$

$$\dot{\tilde{X}}(t) = -L \tilde{\alpha}(1, t). \quad (49)$$

The following Lemma and Remark are also taken from [13].

Lemma 3 ([13, Lemma 7]): Let $L < 0$. Then, the origin of (47)–(49) is exponentially stable in the norm

$$\left(|\tilde{X}(t)|^2 + \int_0^1 \tilde{\alpha}^2(x, t) dx \right)^{\frac{1}{2}}. \quad (50)$$

Remark 4: In view of the dynamics of $\tilde{\beta}$ and the properties of the transformation (30), (31), exponential stability of the origin of (47)–(49) in the norm (50) implies exponential stability of the origin of (25)–(29) in the norm

$$\|(\tilde{\chi}, \tilde{u}, \tilde{v})\|^2 = |\tilde{\chi}(t)|^2 + \int_0^1 (\tilde{u}^2(x, t) + \tilde{v}^2(x, t)) dx. \quad (51)$$

In addition to convergence to 0 in $L_2([0, 1])$, the following can be stated for the boundary errors.

Lemma 5: Let $L < 0$. Then, $\tilde{u}(0, t) \rightarrow 0$ and $\tilde{v}(0, t) \rightarrow 0$ as $t \rightarrow \infty$.

Proof: It is clear from (41) and (43) that $\tilde{\beta}(0, t) \rightarrow 0$ in finite time. Thus, from (42), $\tilde{\alpha}(0, t) \rightarrow \tilde{\chi}$. So, from Lemma 3, $\tilde{\alpha}(0, t) \rightarrow 0$. The result then follows from (30), (31), the boundedness of $(P^{uu}, P^{uv}, P^{vu}, P^{vv})$, the convergence of \tilde{u} and \tilde{v} to 0 in $L_2([0, 1])$ and the boundedness of the domain (which implies convergence in $L_1([0, 1])$). ■

In view of (45), (46), the solution to (32) and (34) with boundary conditions (36) and (38) is needed to compute the output injection gains. Defining

$$c = -\frac{F}{2\rho}, \quad \epsilon = \frac{1}{l} \sqrt{\frac{\beta}{\rho}} \quad (52)$$

the equation becomes

$$\epsilon P_x^{uu}(x, \xi) + \epsilon P_\xi^{uu}(x, \xi) = c e^{-2\frac{\epsilon}{l}x} P^{vu}(x, \xi) \quad (53)$$

$$\epsilon P_x^{vv}(x, \xi) - \epsilon P_\xi^{vv}(x, \xi) = -c e^{2\frac{\epsilon}{l}x} P^{uu}(x, \xi) \quad (54)$$

on $\mathcal{T}_o = \{(x, \xi) : 0 \leq x \leq \xi \leq 1\}$ with boundary conditions

$$P^{uu}(0, \xi) = -P^{vu}(0, \xi) \quad (55)$$

$$P^{vu}(x, x) = -\frac{c}{2\epsilon} e^{2\frac{\epsilon}{l}x}. \quad (56)$$

In [19], an equation equivalent to (53)–(56) was solved in closed form.

Lemma 6: The equation

$$\epsilon K_x^{vu}(x, \xi) - \epsilon K_\xi^{vu}(x, \xi) = ce^{2\frac{\epsilon}{\epsilon}} K^{vu}(x, \xi) \quad (57)$$

$$\epsilon K_x^{vv}(x, \xi) + \epsilon K_\xi^{vv}(x, \xi) = ce^{-2\frac{\epsilon}{\epsilon}} K^{vv}(x, \xi) \quad (58)$$

on $\mathcal{T} = \{(x, \xi) : 0 \leq \xi \leq x \leq 1\}$ with boundary conditions

$$K^{vu}(x, x) = -\frac{c}{2\epsilon} e^{2\frac{\epsilon}{\epsilon}} x \quad (59)$$

$$K^{vv}(x, 0) = -K^{vu}(x, 0) \quad (60)$$

has the unique solution

$$K^{vu}(x, \xi) = -\frac{1}{2\epsilon} \exp\left[\frac{c}{\epsilon}(x + \xi)\right] \left\{ cI_0 \left[\frac{|c|}{\epsilon} \sqrt{(x^2 - \xi^2)} \right] - |c| \sqrt{\frac{x - \xi}{x + \xi}} I_1 \left[\frac{|c|}{\epsilon} \sqrt{(x^2 - \xi^2)} \right] \right\} \quad (61)$$

$$K^{vv}(x, \xi) = \frac{1}{2\epsilon} \exp\left[\frac{c}{\epsilon}(x - \xi)\right] \left\{ cI_0 \left[\frac{|c|}{\epsilon} \sqrt{(x^2 - \xi^2)} \right] - |c| \sqrt{\frac{x + \xi}{x - \xi}} I_1 \left[\frac{|c|}{\epsilon} \sqrt{(x^2 - \xi^2)} \right] \right\} \quad (62)$$

where I_n is the modified Bessel function of the first kind of order n .

Proof: The result is obtained from equations (82)–(83) in [19] by making the substitutions $\epsilon_1 := \epsilon_2 := \epsilon$, $c_1 := c_2 := c_3 := c_4 := c$, and $q := -1$. (Notice that the equation numbers (82)–(83) here refer to equations that are stated in paper [19], and in which the symbols ϵ_1 , ϵ_2 , c_1 , c_2 , c_3 , c_4 , and q appear). ■

Corollary 7: The equation (53), (54) on $\mathcal{T}_o = \{(x, \xi) : 0 \leq x \leq \xi \leq 1\}$ with boundary conditions (55), (56) has the unique solution

$$P^{vu}(x, \xi) = -\frac{1}{2\epsilon} \exp\left[\frac{c}{\epsilon}(\xi + x)\right] \left\{ cI_0 \left[\frac{|c|}{\epsilon} \sqrt{\xi^2 - x^2} \right] - |c| \sqrt{\frac{\xi - x}{\xi + x}} I_1 \left[\frac{|c|}{\epsilon} \sqrt{\xi^2 - x^2} \right] \right\} \quad (63)$$

$$P^{uv}(x, \xi) = \frac{1}{2\epsilon} \exp\left[\frac{c}{\epsilon}(\xi - x)\right] \left\{ cI_0 \left[\frac{|c|}{\epsilon} \sqrt{\xi^2 - x^2} \right] - |c| \sqrt{\frac{\xi + x}{\xi - x}} I_1 \left[\frac{|c|}{\epsilon} \sqrt{\xi^2 - x^2} \right] \right\}. \quad (64)$$

Proof: The result follows from Lemma 6 by substituting $\xi := \bar{x}$, $x := \bar{\xi}$, $K^{vu}(x, \xi) := P^{vu}(\bar{x}, \bar{\xi})$, and $K^{vv}(x, \xi) := P^{uv}(\bar{x}, \bar{\xi})$ into (57)–(60), which gives (53)–(56). Alternatively, the expression (63), (64) can be substituted into (53)–(56) to verify that it is a solution. ■

Summarizing the results, we obtain the main result on leak detection and size estimation.

Theorem 8: Consider the observer (19)–(23) and let the output injection gains be given as

$$p_1(x) = -L - \frac{1}{2} \exp\left[\frac{c}{\epsilon}(1 - x)\right] \left\{ cI_0 \left[\frac{|c|}{\epsilon} \sqrt{1 - x^2} \right] - |c| \sqrt{\frac{1 + x}{1 - x}} I_1 \left[\frac{|c|}{\epsilon} \sqrt{1 - x^2} \right] \right\} + \frac{L}{2\epsilon} \int_x^1 \exp\left[\frac{c}{\epsilon}(\xi - x)\right] \left\{ cI_0 \left[\frac{|c|}{\epsilon} \sqrt{\xi^2 - x^2} \right] - |c| \sqrt{\frac{\xi + x}{\xi - x}} I_1 \left[\frac{|c|}{\epsilon} \sqrt{\xi^2 - x^2} \right] \right\} d\xi \quad (65)$$

TABLE I
PARAMETER VALUES FOR SIMULATION CASE

β	A	ρ	F	l	L	γ
2.2×10^9	0.95	1000	50	24×10^3	-1	0.1

$$p_2(x) = \frac{1}{2} \exp\left[\frac{c}{\epsilon}(1 + x)\right] \left\{ cI_0 \left[\frac{|c|}{\epsilon} \sqrt{1 - x^2} \right] - |c| \sqrt{\frac{1 - x}{1 + x}} I_1 \left[\frac{|c|}{\epsilon} \sqrt{1 - x^2} \right] \right\} - \frac{L}{2\epsilon} \int_x^1 \exp\left[\frac{c}{\epsilon}(\xi + x)\right] \left\{ cI_0 \left[\frac{|c|}{\epsilon} \sqrt{\xi^2 - x^2} \right] - |c| \sqrt{\frac{\xi - x}{\xi + x}} I_1 \left[\frac{|c|}{\epsilon} \sqrt{\xi^2 - x^2} \right] \right\} d\xi \quad (66)$$

and $L < 0$. Then the origin of (25)–(29) is exponentially stable in the norm

$$\|(\tilde{\chi}, \tilde{u}, \tilde{v})\|^2 = |\tilde{\chi}(t)|^2 + \int_0^1 (\tilde{u}^2(x, t) + \tilde{v}^2(x, t)) dx. \quad (67)$$

Moreover, $\tilde{u}(0, t) \rightarrow 0$ and $\tilde{v}(0, t) \rightarrow 0$ as $t \rightarrow \infty$.

Remark 9: Notice that (19)–(23) is independent of the distribution of the leak. That is, leak detection and estimation of its size can be done regardless of where the leak occurs or how it is distributed (single or multiple leaks). While this fact comes as no surprise in the stationary case, where the leak simply equals the in-flow minus the out-flow, it is a nontrivial result for the transient case.

B. Localization

Estimation of the leak location becomes a relatively easy task now that we have at our disposal a leak size estimate that is obtained independently from the leak location. Leak location is found by exploiting discrepancies between inlet pressure estimate and actual inlet pressure, that remain despite the convergence results of the leak size estimation algorithm. The following theorem states the main result on leak localization.

Theorem 10: Define

$$\hat{p}_0(t) = \frac{\sqrt{\beta\rho}}{A} (\hat{u}(0, t) - \hat{v}(0, t)) + p_{out} + \frac{\rho}{A^2} \hat{\chi}(t)^2 + \frac{F}{A} \hat{\delta}(t) \hat{\chi}(t) \quad (68)$$

$$\dot{\hat{\delta}}(t) = \text{proj}_{[0, l]} \{ \gamma (p_0(t) - \hat{p}_0(t)) \} \quad (69)$$

with $\gamma > 0$, and suppose $\chi > 0$ and $F > 0$. Then, $\hat{\delta}(t) \rightarrow \delta(0)$ as $t \rightarrow \infty$.

Proof: From (9), (10), we have

$$u(0, t) = \frac{1}{2} \left(q(0, t) - q_{in} + \delta'(0) \chi + \frac{A}{\sqrt{\beta\rho}} \left(p(0, t) - p_{out} + \frac{\rho}{A^2} \delta'(0) \chi^2 - \frac{F}{A} \delta(0) \chi \right) \right), \quad (70)$$

$$v(0, t) = \frac{1}{2} \left(q(0, t) - q_{in} + \delta'(0) \chi - \frac{A}{\sqrt{\beta\rho}} \left(p(0, t) - p_{out} + \frac{\rho}{A^2} \delta'(0) \chi^2 - \frac{F}{A} \delta(0) \chi \right) \right). \quad (71)$$

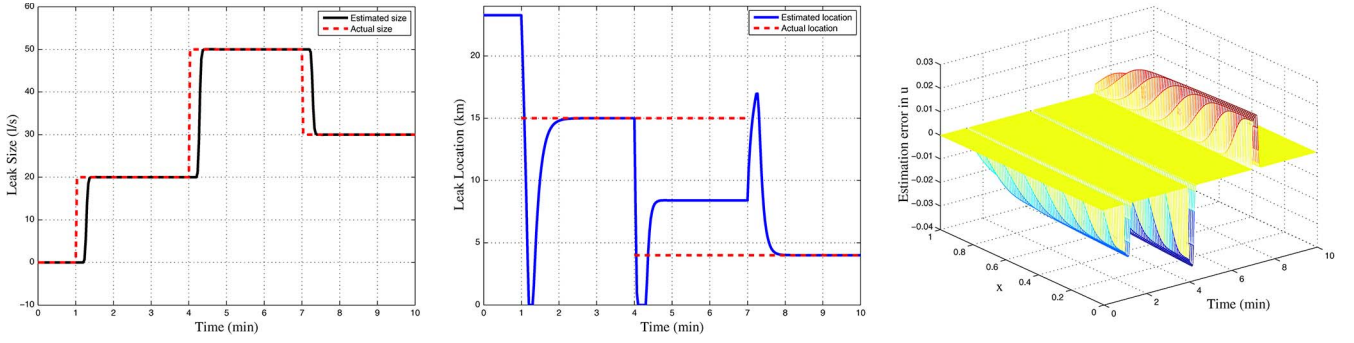


Fig. 1. Estimated and actual total leak size (left graph), estimated and actual leak location(s) (middle graph), and state estimation error, $\tilde{u}(x, t)$ (right graph).

Subtracting (71) from (70), we obtain

$$u(0, t) - v(0, t) = \frac{A}{\sqrt{\beta\rho}} \left(p(0, t) - p_{out} + \frac{\rho}{A^2} \delta'(0) \chi^2 - \frac{F}{A} \delta(0) \chi \right). \quad (72)$$

Since $\delta'(0) = -1$, we get

$$u(0, t) - v(0, t) = \frac{A}{\sqrt{\beta\rho}} \left(p(0, t) - p_{out} - \frac{\rho}{A^2} \chi^2 - \frac{F}{A} \delta(0) \chi \right) \quad (73)$$

and so

$$p_0(t) = \frac{\sqrt{\beta\rho}}{A} (u(0, t) - v(0, t)) + p_{out} + \frac{\rho}{A^2} \chi^2 + \frac{F}{A} \delta(0) \chi. \quad (74)$$

Using (68), we have

$$p_0(t) - \hat{p}_0(t) = \frac{F}{A} \chi (\delta(0) - \hat{\delta}(t)) + \frac{\sqrt{\beta\rho}}{A} (\tilde{u}(0, t) - \tilde{v}(0, t)) + \left(\frac{\rho}{A^2} (\chi + \hat{\chi}(t)) + \frac{F}{A} \hat{\delta}(t) \right) \tilde{\chi}(t). \quad (75)$$

Since $\delta(0) \in (0, l)$, Theorem 8 ensures the existence of T such that

$$\begin{aligned} \frac{F}{A} \chi \delta(0) &> \frac{\sqrt{\beta\rho}}{A} (\tilde{u}(0, t) - \tilde{v}(0, t)) \\ &+ \left(\frac{\rho}{A^2} (\chi + \hat{\chi}(t)) + \frac{F}{A} \hat{\delta}(t) \right) \tilde{\chi}(t), \quad \forall t > T \end{aligned} \quad (76)$$

$$\begin{aligned} \frac{F}{A} \chi (\delta(0) - l) &< \frac{\sqrt{\beta\rho}}{A} (\tilde{u}(0, t) - \tilde{v}(0, t)) \\ &+ \left(\frac{\rho}{A^2} (\chi + \hat{\chi}(t)) + \frac{F}{A} \hat{\delta}(t) \right) \tilde{\chi}(t), \quad \forall t > T \end{aligned} \quad (77)$$

which imply that the projection in (69) is inactive for all $t > T$. Thus, for $t > T$, we have

$$\begin{aligned} \frac{d}{dt} \left\{ \frac{1}{2} \left(\hat{\delta}(t) - \delta(0) \right)^2 \right\} &= -\gamma \frac{F}{A} \chi \left(\hat{\delta}(t) - \delta(0) \right)^2 + \gamma \left(\hat{\delta}(t) - \delta(0) \right) \\ &\times \left(\frac{\sqrt{\beta\rho}}{A} (\tilde{u}(0, t) - \tilde{v}(0, t)) + \left(\frac{\rho}{A^2} (\chi + \hat{\chi}) + \frac{F}{A} \hat{\delta} \right) \tilde{\chi} \right) \end{aligned} \quad (78)$$

which provides the result in view of Theorem 8. \blacksquare

Remark 11: Equation (78) clearly reveals the conditions under which localization is possible. In fact, the convergence rate of the location estimate is proportional to the size of the leak and the amount of friction loss in the pipe. It is worth noting that not only the leak size estimation is independent of the leak distribution $d(z)$. The estimation

of the leak location in terms of $\delta(0)$ is independent of the distribution, too. As long as there is a leak, and there is friction, an estimate of $\delta(0)$ can be obtained. The relation between $\delta(0)$ and the distribution $d(z)$ is not unique, though, but additional assumptions about the distribution can be used to deduce accurate localisation results, as shown next.

The quantity $\delta(0)$ depends on the distribution of the leak over the pipeline, as defined by $d(z)$ which has properties given by (4). For point-leaks, the locations of the leaks are well defined, and we can state the following.

Corollary 12: Suppose there is a point-leak at location $z^* \in (0, l)$. Then, $\hat{\delta}(t) \rightarrow z^*$ as $t \rightarrow \infty$.

Proof: Pick any $\Delta > 0$ such that $(z^* - \Delta, z^* + \Delta) \in (0, l)$. Since the leak is assumed to be a point-leak, we have

$$\int_0^\eta d(\gamma) d\gamma = 0 \quad \forall \eta \in [0, z^* - \Delta] \quad (79)$$

$$\int_0^\eta d(\gamma) d\gamma = 1 \quad \forall \eta \in [z^* + \Delta, l]. \quad (80)$$

It follows that

$$\delta(0) = z^* + \Delta - \int_{z^* - \Delta}^{z^* + \Delta} \int_0^\eta d(\gamma) d\gamma d\eta < z^* + \Delta. \quad (81)$$

Furthermore

$$\begin{aligned} \delta(0) &= z^* + \Delta - \int_{z^* - \Delta}^{z^* + \Delta} \int_0^\eta d(\gamma) d\gamma d\eta \\ &> z^* + \Delta - \int_{z^* - \Delta}^{z^* + \Delta} 1 d\eta = z^* - \Delta. \end{aligned} \quad (82)$$

It follows that $\hat{\delta}(t) \rightarrow (z^* - \Delta, z^* + \Delta)$. Since Δ was arbitrary, $\hat{\delta}(t) \rightarrow z^*$. \blacksquare

The following can be shown in a similar manner, for the event of two point-leaks.

Corollary 13: Suppose there are two point-leaks, with sizes $\chi_1 > 0$ and $\chi_2 > 0$ at locations $0 < z_1^* < z_2^* < l$. Then

$$\hat{\delta}(t) \rightarrow \frac{\chi_1}{\chi_1 + \chi_2} z_1^* + \frac{\chi_2}{\chi_1 + \chi_2} z_2^* \quad (83)$$

as $t \rightarrow \infty$.

IV. SIMULATIONS

To illustrate the results from the previous sections, a water supply pipeline of realistic dimensions is simulated. The simulations of the infinite-dimensional observer equations are carried out using first order finite differences on a uniform grid of 200 nodes for the spatial discretization, and MATLAB's ode45 for time integration (a more efficient method of spatial discretization is developed in [20]). The pipeline is 24 km long and has an inner diameter of 1.1 m. Parameters used for simulation are summarized in Table I. The inlet flow and outlet pressure are set to vary to create transient conditions in the pipeline. Fig. 1 compares the estimated leak size and location to their actual values. The observer is run for a while prior to any leak occurring, so that state estimates have converged to their true values at $t = 0$. At $t = 1$ minute, a point leak of 20 l/s occurs 15 km from the pipe inlet. Then, at $t = 4$ minutes, a second leak occurs 4 km from the pipe inlet. It has size 30 l/s, bringing the total leak size up to 50 l/s. At $t = 7$ minutes, the first leak is fixed. The left graph shows that the leak size is estimated correctly very quickly. The middle graph shows that the location is estimated correctly when there is a single leak (prior to $t = 4$ and after $t = 7$). When there are two leaks, the location is estimated to be between the leaks according to (83). Of course, the correct location of the second leak can be computed at, for instance, $t = 5$ minutes, by solving (83) for z_2^* using the graphs to let $\chi_1 = \hat{\chi}(3)$, $\chi_1 + \chi_2 = \hat{\chi}(5)$, $z_1^* = \hat{\delta}(3)$ and $\hat{\delta}(t) = \hat{\delta}(5)$. The error in the observer state estimate $\tilde{u}(x, t)$ is shown in the right graph (the error $\tilde{v}(x, t)$ looks qualitatively the same). The states converge quickly to their true values as the leak size is estimated correctly. The simulations are carried out under ideal conditions, and merely provide a numerical confirmation of the theoretical results. It remains to test the results experimentally.

REFERENCES

- [1] P.-S. Murvay and I. Silea, "A survey on gas leak detection and localization techniques," *J. Loss Prevent. Process Ind.*, vol. 25, pp. 966–973, 2012.
- [2] L. Billmann and R. Isermann, "Leak detection methods for pipelines," *Automatica*, vol. 23, no. 3, pp. 381–385, 1987.
- [3] C. Verde, "Multi-leak detection and isolation in fluid pipelines," *Control Eng. Pract.*, vol. 9, pp. 673–682, 2001.
- [4] M. Hou and P. Müller, "Fault detection and isolation observers," *Int. J. Control*, vol. 60, no. 5, pp. 827–846, 1994.
- [5] J. Salvesen, "Leak detection by estimation in an oil pipeline," M.Sc. thesis, NTNU, Trondheim, Norway, 2005.
- [6] C. Verde, "Minimal order nonlinear observer for leak detection," *J. Dynam. Syst., Measur., Control*, vol. 126, pp. 467–472, 2004.
- [7] O. M. Aamo, J. Salvesen, and B. A. Foss, "Observer design using boundary injections for pipeline monitoring and leak detection," in *Proc. Int. Symp. Adv. Control Chem. Process.*, Gramado, Brazil, Apr. 2–5, 2006, pp. 53–58.
- [8] E. Hauge, O. M. Aamo, and J.-M. Godhavn, "Model based pipeline monitoring with leak detection," in *Proc. 7th IFAC Symp. Nonlinear Control Syst.*, Pretoria, South Africa, Aug. 22–24, 2007, pp. 318–323.
- [9] E. Hauge, O. M. Aamo, and J.-M. Godhavn, "Model-based monitoring and leak detection in oil and gas pipelines," *SPE Projects, Facil. Construct.*, vol. 4, no. 3, pp. 53–60, 2009.
- [10] K. Hodne, "Leak detection in two-phase oil and gas pipelines by parameter- and state estimation," M.Sc. thesis, NTNU, 2008.
- [11] R. Vazquez, M. Krstic, and J.-M. Coron, "Backstepping boundary stabilization and state estimation of a 2×2 linear hyperbolic system," in *Proc. 50th IEEE Conf. Decision Control Eur. Control Conf.*, Orlando, FL, USA, 2011, pp. 4937–4942.
- [12] M. Krstic and A. Smyshlyaev, "Backstepping boundary control for first-order hyperbolic PDEs and application to systems with actuator and sensor delay," *Syst. Control Lett.*, vol. 57, pp. 750–758, 2008.
- [13] O. M. Aamo, "Disturbance rejection in 2×2 linear hyperbolic systems," *IEEE Trans. Autom. Control*, vol. 58, no. 5, pp. 1095–1106, May 2013.
- [14] N. Bedjaoui and E. Weyer, "Algorithms for leak detection, estimation, isolation and localization in open water channels," *Control Eng. Pract.*, vol. 19, pp. 564–573, 2011.
- [15] E. Hauge, O. M. Aamo, J.-M. Godhavn, and G. Nygaard, "A novel model-based scheme for kick and loss mitigation during drilling," *J. Process Control*, vol. 23, no. 4, pp. 463–472, 2013.
- [16] E. Hauge, O. M. Aamo, and J.-M. Godhavn, "Application of an infinite-dimensional observer for drilling systems incorporating kick and loss detection," in *Proc. Eur. Control Conf.*, Zurich, Switzerland, Jul. 17–19, 2013, pp. 1065–1070.
- [17] J. Zhou, Ø. N. Stamnes, O. M. Aamo, and G.-O. Kaasa, "Switched control for pressure regulation and kick attenuation in a managed pressure drilling system," *IEEE Trans. Control Syst. Technol.*, vol. 19, no. 2, pp. 337–350, 2011.
- [18] O. Egeland and J. T. Gravdahl, "Modeling and simulation for automatic control," *Marine Cybernetics*, 2002.
- [19] R. Vazquez and M. Krstic, "Marcum Q-functions and explicit kernels for stabilization of 2×2 linear hyperbolic systems with constant coefficients," *Syst. Control Lett.*, vol. 68, pp. 33–42, 2014.
- [20] H. Anfinson and O. M. Aamo, "A model reduction algorithm for irrational transfer functions with application to leak detection in pipelines," in *Proc. Amer. Control Conf.*, Chicago, IL, USA, Jul. 1–3, 2015.